Available online at www.sciencedirect.com
ScienceDirect
International Journal of Multiphase Flow 34 (2008) 1185–1189
International Journal of Multiphase Flow
www.elsevier.com/locate/ijmulflow

Brief Communication

Effect of startup conditions on drop breakup under shear with inertia

Yuriko Renardy *,[1]

Department of Mathematics, Virginia Tech, 460 McBryde Hall, Blacksburg, VA 24061-0123, USA

Received 29 February 2008; received in revised form 16 April 2008; accepted 21 April 2008
Available online 13 June 2008

1. Introduction

The model problem of a single droplet sheared between parallel walls is of interest in the processing of dilute suspensions for which coalescence is negligible, and equilibrium drop sizes are determined at breakup (Bigio et al., 1998; Scardovelli and Zaleski, 1999; Paul et al., 2003; Fischer and Erni, 2007). Drop deformation under shear in Stokes flow has recently been simulated with a number of methods: the boundary integral method (Cristini et al., 1998, 2003; Bazhlekov et al., 2006), spectral algorithms (Yechun and Dimitrakopoulos, 2006; Dimitrakopoulos, 2007), front-tracking methods (Popinet and Zaleski, 1999; Aggarwal and Sarkar, 2007; Muradoglu and Tryggvason, 2008), the level set method (Pillapakkam and Singh, 2001), finite element method (Hooper et al., 2001), diffuse interface method (Yue et al., 2005), and the volume-of-fluid method (Lafaurie et al., 1994; Li et al., 2000; Renardy and Renardy, 2002). In addition, the latter method has been used to examine the first effects of inertia (Renardy et al., 2002), and this paper focusses on this regime. It is well known that the uniqueness associated with Stokes flow is lost when inertia is included. In particular, an analysis of the initial overshoot, and its extent associated with initial conditions, is examined.

2. Formulation

The two liquids are governed by the Navier–Stokes equations and incompressibility. At the interface between the drop and the surrounding liquid, the jump in the normal stress is balanced by surface tension, and velocity and shear stress are continuous. At the top and bottom boundaries, the walls move to provide shear. Spatial periodicity is assumed in the horizontal x and y directions. The domain (see Fig. 1) is taken sufficiently large so that neighboring drop interactions are minimal.

In Stokes flow, the viscous force in the surrounding liquid deforms the drop while the capillary force stabilizes it. These competing forces are expressed by the capillary number $Ca = \mu_m \dot{\gamma} a/\sigma$, where a denotes the initial radius of the drop, $\dot{\gamma}$ is the shear rate, μ_m the viscosity of the surrounding liquid, and σ the interfacial tension parameter. The relative importance of inertial to viscous effects is expressed by the Reynolds number, $Re = \rho_m \dot{\gamma} a^2/\mu_m$, where ρ_m denotes the density of the surrounding liquid. The drop and matrix liquids are assumed to have equal densities to avoid buoyancy effects, and may have different viscosities μ_d and μ_m. The drop to matrix viscosity ratio is denoted $\lambda = \mu_d/\mu_m$. In the following, t denotes the dimensionless time with respect to the shear rate $\dot{\gamma}$.

The Grace curve (Grace, 1982; Stegeman et al., 2002) is an experimentally determined curve for Stokes flow that gives the relation between the critical capillary number (below which the drop reaches stationary state and above which the drop breaks up) and the viscosity ratio for the breakup of an initially spherical droplet. This curve is often used to find an optimal flow rate in industrial mixers. Given the droplet size, the curve can be used to find the shear rate that is needed. Data for this are obtained by increasing the flow rate until drop breakup is observed (Guido and Villone, 1998; Guido and Greco, 2001). To obtain the Grace curve numerically, the viscosity ratio is prescribed and the capillary number is increased until breakup occurs. Cristini et al. (2003) shows that the critical capillary number approaches infinity at $\lambda = 0$ and $\lambda > \lambda^* \approx 3$. For viscosity ratios greater than λ^*, the drop evolves to a steady shape for all capillary numbers. On the other hand, inertia increases the suction provided

* Tel.: +1 540 320 1573.
E-mail address: renardyy@aol.com
URL: http://www.math.vt.edu/people/renardyy.

[1] Supported by NSF DMS 0456086, NCSA CTS060022 and the Virginia Tech ARC SGI supercluster. The author thanks K. Verhulst, S. Afkhami and the Moldenaers group (KU Leuven) for stimulating discussions.

doi:10.1016/j.ijmultiphaseflow.2008.04.004

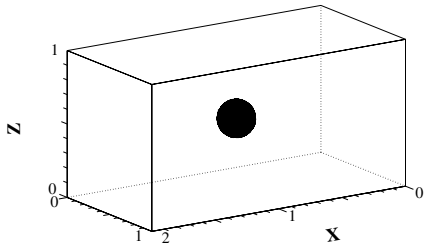

Fig. 1. Initial configuration for direct numerical simulation.

by the pressures generated near the drop tips, thus tilting the drop further (de Bruijn, 1989; Guido and Greco, 2001). The addition of inertia shifts the value of λ^* to above 3; thus, drops can be broken for a wider range of viscosity ratios (Khismatullin et al., 2003). Theoretical results on the effect of inertia on criticalities are few compared with those on Stokes flow (Stone, 1994; Sheth and Pozrikidis, 1995; Renardy and Cristini, 2001a; Renardy et al., 2002; Renardy and Cristini, 2001b; Khismatullin et al., 2003). The goal of this brief communication is to illustrate a capillary number at which the drop breaks for the abrupt initial condition but does not for a gentle initial condition.

3. Numerical results

Direct numerical simulations are performed with a three-dimensional transient volume-of-fluid (VOF) continuum surface force (CSF) method. The spatial discretization is a regular Cartesian mesh. The location of the two liquids are defined by a color function per mesh cell, equal to the volume fraction of the drop liquid. This function is advected with the flow in a Lagrangian manner. The discretized velocity and pressure are staggered. The color function is discretized at the same location as pressure. Time integration is semi-implicit, with an operator factorization. The interface location is reconstructed from the color function with the piecewise linear interface construction scheme (PLIC). Implementation and tests are detailed in Li et al. (2000), Renardy et al., 2002, in which the initial condition is a spherical drop placed in an established background shear. On the other hand, comparison with experimental data begin with a drop in a parallel plate device from rest. This raises the question of the influence of initial conditions on the critical curve for breakup in the presence of inertia.

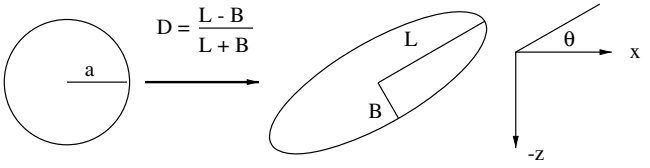

Fig. 2. Sideview deformation and orientation.

The computational domain is the rectangular box of Fig. 1; it is bounded above and below by plates that move to generate a shear rate $\dot{\gamma}$ in the bulk of the outer liquid, with the plate separation $8a$ to eliminate wall effects. Periodic boundary conditions apply in the horizontal x and y directions, also at least $8a$ apart to prevent neighboring drop interactions for the parameters below. Fig. 2 shows the definition of the Taylor deformation D in terms of the half-length L and half-breadth B, both dimensionless with respect to the drop radius a. The drop is observed from the side, i.e., projected to the $x-z$ plane.

A gentle startup condition is a spherical drop placed in a flow at rest after which the walls move to start the shear, as in Fig. 3(a). This shows the velocity of the walls penetrating into the bulk of the fluid in finite time. In the figure, the viscous shear is yet to arrive at the drop. An abrupt startup condition is a drop placed in an established shear flow as in Fig. 3(b). Stokes flow is not sensitive to the difference between figures (a) and (b) because of the instantaneous smoothing of data for elliptic PDEs; the motion of the walls is instantly felt through the whole domain. Inertia prevents this and when the walls begin to move, wall shear takes time to propagate to the drop.

In what follows, the case of viscosity ratio 1 is addressed, at a shear rate that yields $Re = 10$, and consider three separate ways to achieve this. One case is ini-

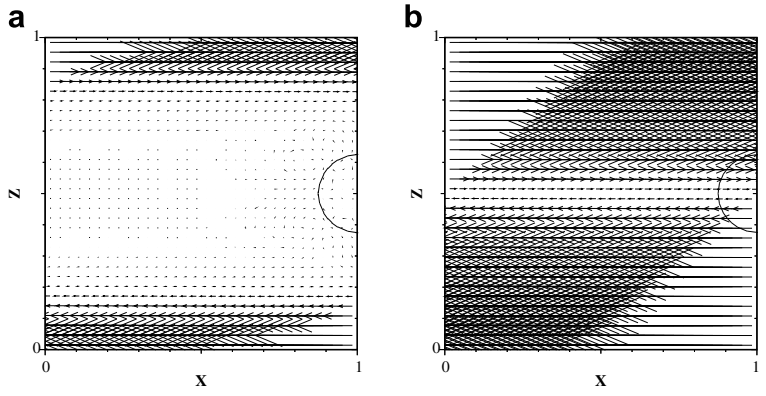

Fig. 3. $Re = 10, Ca = 0.15$. Velocity vector plot in the x–z cross-section through the center of the drop (a) when the upper and lower walls are set into motion from zero flow, $t = 2$; (b) the drop is initially placed in an established shear flow $t = 0$.

tially zero velocity after which the plates move at the shear rate that corresponds to $Re = 10$, as in Fig. 3(a). This is the most physically realizable case of the three initial conditions. The second case is initially uniform shear with the plate speeds producing $Re = 10$ as in Fig. 3(b). Under experimental conditions, it is usually not possible to place a spherical drop in an established shear flow. The third case is to start at uniform shear at a low Reynolds number such as $Re = 2$, also as in Fig. 3(b), let the drop reach a steady state shape, and increase the plate speeds in steps $(Re = 2, 4, 6, 8, 10)$ every time a stationary shape is achieved until the plate speeds match $Re = 10$. Sideview drop deformation is examined; that is, in the x–z cross-section through the center of the drop. The center of the drop and the interface node farthest away are used to define the half-length L. The distance from the closest interface node to the center of the drop defines a half-breadth B. The half-length vector subtends an angle of orientation θ with the x-direction.

Fig. 4 shows the evolution of the half-breadth B and angle of tilt θ to the direction of flow, *vs.* dimensionless time. Oscillations are clearly seen here for the case of an abrupt start at $Re = 10$ (-.-). This begins with a spherical drop in established shear, an initial condition which is typically used for modeling Stokes flow in an unbounded domain. Under experimental conditions, it is not feasible to place a spherical drop in established shear. The oscillations, or wobbling, are not observed in the angle of tilt. The bold line in Fig. 4 (—) starts with the spherical drop placed in established shear at the lower shear rate $Re = 2$. There is an oscillation here which is smaller in magnitude, as it is lower in inertia. The dashed line shows the mildest distortion; this models a parallel plate device with a drop in zero flow followed by impulsively started walls at the shear rate for $Re = 10$. The wild variation in θ here up to $t = 4$ is numerical error, due to the almost

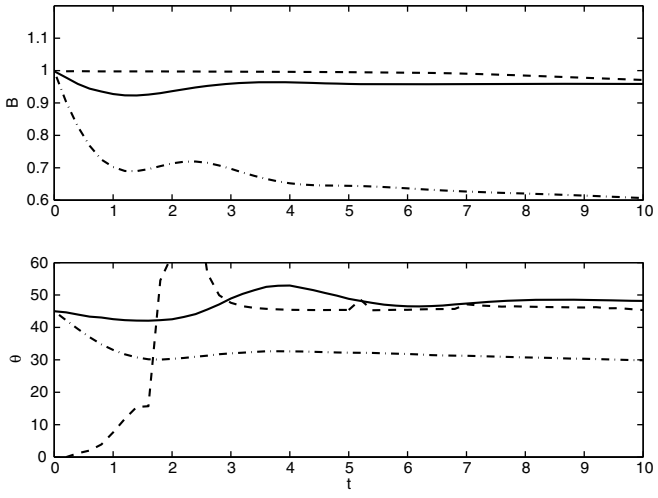

Fig. 4. Initial transients for half-breadth B vs t, angle θ vs t for three cases; initial drop in established shear at $Re = 2, Ca = 0.031$ (—); at $Re = 10, Ca = 0.15$ (-.-.) shown with sideview drop shapes; initial drop in zero flow followed by wall motion at $Re = 10$ (- - -) shown with drop shape at maximal extension.

spherical drop, and therefore the angle being essentially indefinite. Once the drop is no longer spherical, the interface node farthest from the drop center is well-defined in the simulations. A typical discretization for $Re = 10, Ca = 0.15$ with initially zero flow is a spatial mesh $\Delta x = \Delta y = \Delta z = a/12$, time step $\Delta t\dot{\gamma} = 0.0005$, and a computational domain of $16a \times 8a \times 8a$.

Fig. 5 shows drop shapes and evolution of the sideview half-length (L) corresponding to Fig. 4. The abrupt start at $Re = 10$ (-.-) has the overshoot which takes the drop to a significant enough deformation that it breaks. The gentle start for $Re = 10$ (- - -) avoids the overshoot, and allows the drop to reach stationary state. The case $Re = 2$ (—) for a drop placed in shear has an overshoot which is not high enough to cause breakup. This case can be used to ramp up to $Re = 10$ without breakup.

Figs. 6 and 7 show the subsequent evolution over a sufficiently large interval of time until either breakup or stationary state is achieved. Fig. 6 shows the deformation D and angle θ of the major axis in the x–z cross-section of the drop. The case of the initially established shear at $Re = 10$ (-.-) breaks up before $t = 50$. The gradual ramping (—) begins at $Re = 2, Ca = 0.031$, then to $Re = 4, Ca = 0.063$ at $t = 20$, to $Re = 6, Ca = 0.094$ at $t = 60$, to $Re = 8, Ca = 0.13$ at $t = 117$, and finally to $Re = 10, Ca = 0.15$ at $t = 192$. The latter shape settles before $t = 300$. The same final stationary state is reached when the overshoot is avoided, whether through gradual ramping of the shear rates (— in Fig. 6) or from an initial state at rest (- - -).

4. Scaling

In Stokes flow, it is known that when the upper and lower plates are moved to establish simple shear, there is an instantaneous response over the entire domain. Below the critical capillary number of approximately 0.43 for vis-

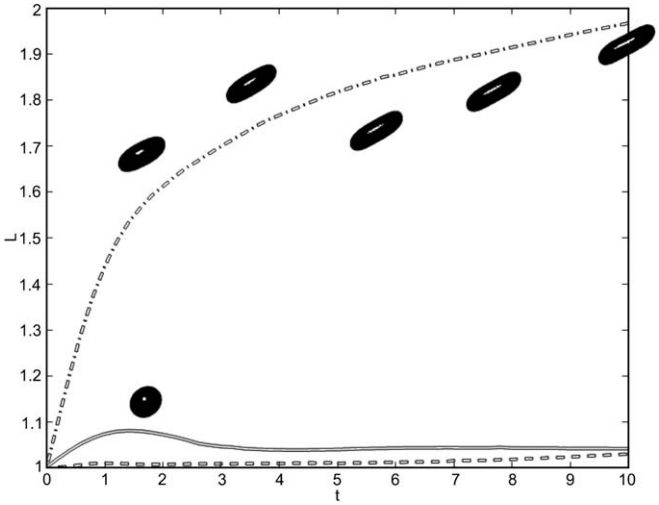

Fig. 5. Initial transients for half-length of the ellipsoidal x–z cross-section L vs t. $Re = 2, Ca = 0.031$ (—); $Re = 10, Ca = 0.15$ (-.-.); in zero flow followed by impulsively started walls (- - -).

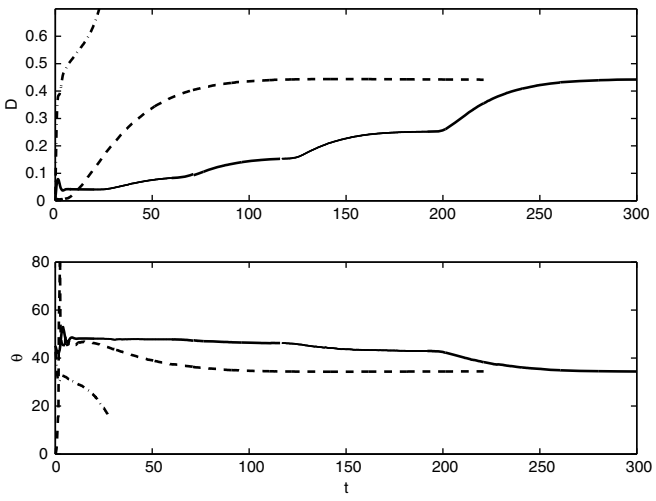

Fig. 6. Evolution to stationary state at $Re = 10, Ca = 0.15$ by ramping up shear rate five times from $Re = 2, Ca = 0.031$ (—); evolution to breakup for drop placed in established shear $Re = 10, Ca = 0.15$ (-.-.); evolution to stationary state from zero flow followed by impulsively started walls (- - -). t is dimensionless with respect to the shear rate at $Re = 10$.

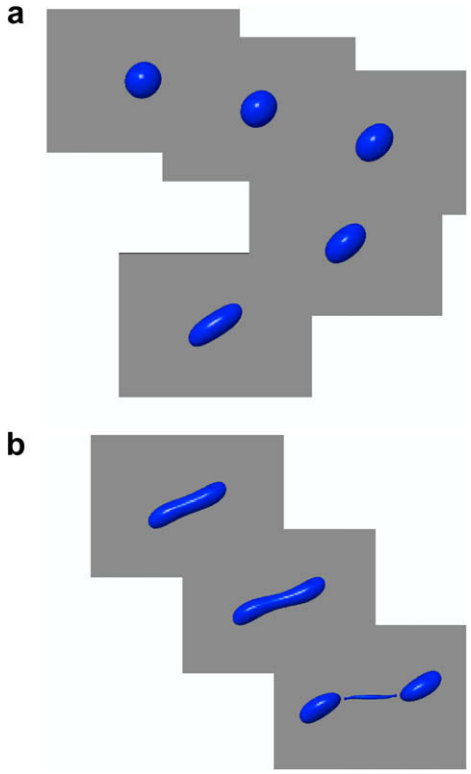

Fig. 7. (a) Drop shapes for Fig. 6 at stationary states when the shear rate is ramped up after the drop settles. The five shapes are $Re = 2$, $Ca = 0.031, t = 20$ (— in Fig. 6); $Ca = 0.0625, Re = 4, t = 60$ (...); $Ca = 0.094, Re = 6, t = 117$ (—); $Ca = 0.126, Re = 8, t = 192$ (...); $Re = 10, Ca = 0.15, t = 300$ (—). The same final shape is reached when the drop and surrounding liquid are at rest, followed by impulsively started walls (- - -, in Fig. 6). (b) Drop shapes for the case of initially established simple shear at $Re = 10, Ca = 0.15$ (-.-. in Fig. 6) at $t = 20, 25, 30$. The drop eventually breaks.

cosity ratio 1 (Cristini et al., 2003), the drop elongates monotonically to a steady shape. On the other hand, when inertia is present, viscous effects take a time scale of $O(Re)$ to propagate the motion of the walls into the interior and reach the drop. This external shear drives the force which deforms the drop and therefore, in the gentle startup scenario, the drop takes a longer time to deform. On the other hand, when the background shear is already present as an initial condition, the drop is immediately forced to deform by inertia, before capillary or viscous effects can act. The drop responds with higher elongation. When this overshoot is sufficient to start the breakup process, then a 'critical capillary number' is attained. On the other hand, if the overshoot is avoided through a gentle startup, the drop can settle to a stationary state at an even higher capillary number. Thus, a critical curve is not unique.

Transient overshoots and oscillations occur naturally at large Reynolds numbers. When inertia is important, larger velocities are induced at the drop tips, tilting the drop higher than in Stokes flow. This lift exposes the drop to larger speeds in the external flow, and a transient wobbling takes place. Renardy and Cristini (2001a) find that close to but just below the critical state, drop evolution at high Reynolds number is described by a one-dimensional damped mass-spring system

$$Re \cdot Ca.x''(t) + Ca.x'(t) + x(t) \sim 0, \tag{1}$$

where $x(t)$ denotes drop breadth. This yields a period of oscillation proportional to $(Re \cdot Ca)^{1/2}$. The decay rate as the drop approaches equilibrium is proportional to $-1/Re$. Oscillations are also present for drops that break. The examples in Section 3 illustrate these features for Reynolds numbers as low as 10 at viscosity ratio 1 (Renardy and Cristini, 2001a).

The effect of startup conditions is modeled next. Let $x = L - a$. The mass is of order ρa^3, the restoring force is of order σx, and the viscous drag force is of order $\mu a\dot{x}$. The external force, if it is dominated by inertia, is of order $F = \rho U^2 a^2$, where $U = a\dot{\gamma}$ is the velocity with which the drop is sheared. This leads to the equation

$$\rho a^3 \ddot{x} + \mu a\dot{x} + \sigma x = \rho U^2 a^2. \tag{2}$$

The equilibrium deformation is

$$x = \rho U^2 a^2/\sigma.$$

The dimensionless deformation is

$$x/a = \rho U^2 a/\sigma = \frac{\rho U a}{\mu}\frac{\mu U}{\sigma} = ReCa.$$

That is, the deformation of the drop, when an equilibrium exists, is of order Re Ca. This scaling is verified for viscosity ratio 1 with calculation of the critical curve for large Re in Fig. 1 of Renardy and Cristini, 2001a.

If the drop is placed into a pre-existing shear flow, the initial conditions are $x(0) = 0$, and $\dot{x}(0)$ is of order U. If damping is small (high Re), these initial conditions will lead to an overshoot. If, on the other hand, the wall is started up

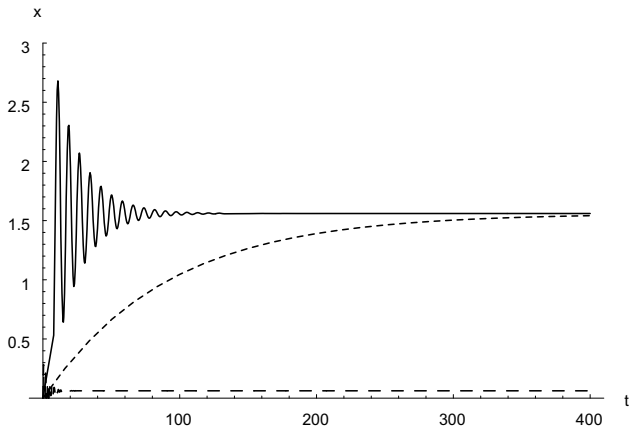

Fig. 8. The three cases in Fig. 6 are qualitatively modeled with (3) or (4). $x = L/a - 1$ *vs* $t\dot{\gamma}$. $\dot{\gamma} = 1$, $Re = 10, Ca = 0.15, t_v = 90$, drop placed in established shear (3) —; drop and outer liquid started from rest (4) - - -; and drop placed in established shear (3) at $Re = 2, Ca = 0.031$, – – –.

with the drop in place, the initial conditions are $x(0) = \dot{x}(0) = 0$. Moreover, the force F is turned on gradually. The time taken to establish the flow is determined by the viscous diffusion time $t_v \sim \rho Z^2/\mu$, where Z is the distance of the drop from the wall. On the other hand, the time scale for damping of the oscillating drop is of order $t_d \sim \rho a^2/\mu$. Since $a \ll Z$, the timescale over which the external force is turned on is long compared to the timescale over which oscillations are damped. This eliminates the overshoot. Moreover, if x is made dimensionless with respect to a and t with $\dot{\gamma}$, then (2) becomes

$$x''(t) + x'(t)/Re + x(t)/Re \cdot Ca = 1, \quad x(0) = 0, \quad x'(0) = 1, \tag{3}$$

for a drop in established shear, and

$$x''(t) + x'(t)/Re + x(t)/Re \cdot Ca = 1 - e^{-t/t_v}, \quad x(0) = 0, \quad x'(0) = 0, \tag{4}$$

for the flow starting from rest. Fig. 8 shows the qualitative features of this model, applied to the three initial conditions in Figs. 6. The drop placed in shear (—) at $Re = 10, Ca = 0.15, t_v = 90, x'(0) = 1, x(0) = 0, x(t)$ displays overshoots which qualitatively describe the breakup in Fig. 6(b), while the one at $Re = 2$ grows more slowly to a much smaller amplitude (– – –) and qualitatively agrees with Fig. 6(a). When the flow is initially at rest ($x(0) = 0, x'(0) = 0$), the forcing on the drop increases during the initial t_v period (- - -) and is analogous to Fig. 6(c). This confirms the *a priori* scaling estimates on the basis of the numerical simulations.

References

Aggarwal, N., Sarkar, K., 2007. Deformation and breakup of a viscoelastic drop in a Newtonian matrix under steady shear. J. Fluid Mech. 584, 1–21.

Bazhlekov, I.B., Anderson, P.D., Meijer, H.E.H., 2006. Numerical investigation of the effect of insoluble surfactants on drop deformation and breakup in simple shear flow. J. Colloid Interface Sci. 298, 369–394.

Bigio, D.I., Marks, C.R., Calabrese, R.V., 1998. Predicting drop breakup in complex flows from model flow experiments. Int. Polym. Process. XIII2, 192–198.

Cristini, V., Blawzdziewicz, J., Loewenberg, M., 1998. Drop breakup in three-dimensional viscous flows. Phys. fluids 10, 1781–1783.

Cristini, V., Guido, S., Alfani, A., Blawzdziewicz, J., Loewenberg, M., 2003. Drop breakup and fragment size distribution in shear flow. J. Rheol. 47, 1283–1298.

de Bruijn, R., 1989. Deformation and breakup of drops in simple shear flows. Ph.D. thesis, Tech. University of Eindhoven.

Dimitrakopoulos, P., 2007. Interfacial dynamics in stokes flow via a three-dimensional fully-implicit interfacial spectral boundary element algorithm. J. Comp. Phys. 225, 408–426.

Fischer, P., Erni, P., 2007. Emulsion drops in external flow fields – The role of liquid interfaces. Curr. Opin. Colloid Interface Sci. 12, 196–205.

Grace, H.P., 1982. Dispersion phenomena in high viscosity immiscible fluid systems and application of static mixers as dispersion devices in such systems. Chem. Eng. Commun. 14, 225–277.

Guido, S., Greco, F., 2001. Drop shape under slow steady shear flow and during relaxation. experimental results and comparison with theory. Rheol. Acta 40, 176–184.

Guido, S., Villone, M., 1998. Three-dimensional shape of a drop under simple shear flow. J. Rheol. 42, 395–415.

Hooper, R., Cristini, V., Shakya, S., Lowengrub, J.S., Macosko, C.W., Derby, J.J., 2001. Modeling multiphase flows using a novel 3d adaptive remeshing algorithm. In: Computational Methods in Multiphase Flow, Advances in Fluid Mechanics, vol. 29. Wessex Institute of Technology Press, UK, pp. 33–42.

Khismatullin, D., Renardy, Y., Cristini, V., 2003. Inertia-induced breakup of highly viscous drops subjected to simple shear. Phys. Fluids 15, 1351–1354.

Lafaurie, B., Nardone, C., Scardovelli, R., Zaleski, S., Zanetti, G., 1994. Modelling merging and fragmentation in multiphase flows with SURFER. J. Comp. Phys. 113, 134–147.

Li, J., Renardy, Y., Renardy, M., 2000. Numerical simulation of breakup of a viscous drop in simple shear flow through a volume-of-fluid method. Phys. Fluids 12, 269–282.

Muradoglu, M., Tryggvason, G., 2008. A front-tracking method for computation of interfacial flows with soluble surfactants. J. Comp. Phys. 227, 2238–2262.

Paul, E.L., Atiemo-Obeng, V., Kresta, S.M. (Eds.), 2003. Handbook of Industrial Mixing: Science and Practice. Wiley Interscience.

Pillapakkam, S.B., Singh, P., 2001. A level-set method for computing solutions to viscoelastic two-phase flow. J. Comp. Phys. 174, 552–578.

Popinet, S., Zaleski, S., 1999. A front-tracking algorithm for the accurate representation of surface tension. Int. J. Numer. Methods Fluids 30, 775–793.

Renardy, Y., Cristini, V., 2001a. Effect of inertia on drop breakup under shear. Phys. Fluids 13, 7–13.

Renardy, Y., Cristini, V., 2001b. Scalings for fragments produced from drop breakup in shear flow with inertia. Phys. Fluids 13, 2161–2164.

Renardy, Y., Cristini, V., Li, J., 2002. Drop fragment distributions under shear with inertia. Int. J. Mult. Flow 28, 1125–1147.

Renardy, Y., Renardy, M., 2002. PROST: a parabolic reconstruction of surface tension for the volume-of-fluid method. J. Comp. Phys. 183, 400–421.

Scardovelli, R., Zaleski, S., 1999. Direct numerical simulation of free surface and interfacial flow. Ann. Rev. Fluid Mech. 31, 567–604.

Sheth, K.S., Pozrikidis, C., 1995. Effect of inertia on the deformation of liquid drops in simple shear flow. Comput. Fluids 24, 101–119.

Stegeman, Y.W., van de Vosse, F.N., Meijer, H.E.H., 2002. On the applicability of the grace curve in practical mixing operations. Can. J. Chem. Eng. 80, 1–6.

Stone, H.A., 1994. Dynamics of drop deformation and breakup in viscous fluids. Ann. Rev. Fluid Mech. 26, 65–102.

Yechun, E., Dimitrakopoulos, P., 2006. A three-dimensional spectral boundary element algorithm for interfacial dynamics in Stokes flow. Phys. Fluids 18, 1–16.

Yue, P., Feng, J.J., Liu, C., Shen, J., 2005. Viscoelastic effects on drop deformation in steady shear. J. Fluid Mech. 540, 427–437.